First European Conference on Earthquake Engineering and Seismology
(a joint event of the 13th ECEE & 30th General Assembly of the ESC)
Geneva, Switzerland, 3-8 September 2012
Paper Number: 793

A COMPARATIVE EVALUATION OF DATA PROCESSING SCHEMES USING TURKISH STRONG GROUND-MOTION DATA

Emrah YENIER[1], Ali Zeynel DENIZOGLU[2], Zahide COLAKOGLU[3] and Sinan AKKAR[4]

SUMMARY

A consistent ground-motion data processing scheme is important for most of the earthquake engineering and engineering seismology related research. Of the various data processing procedures filtering is the most implemented technique in removing the low- and high-frequency noise from the strong motion data. Two different filtering approaches for removing the low-frequency noise are investigated in this study. One of these approaches is based on the noise information revealed by the fixed trace of analogue records whereas the other approach uses an iterative scheme associated with the guidance of theoretical source spectra to determine the low-cut filter frequency (f_c). The objective of this study is two folded: (a) to observe the differences and similarities of low-cut filter frequencies computed from these two approaches, (b) to observe the influence of f_c values determined from these approaches on peak ground-motion values and elastic and inelastic spectral displacement ordinates.

1. INTRODUCTION

The raw ground-motion records generally contain high- and low-frequency noise that should be eliminated before their use in engineering and seismological studies. Filtering is one of the most preferred ground-motion processing techniques that removes the high- and low-frequency noise from the unprocessed data. The choice of filter cut-off frequencies is the essential and the most challenging part of the filtering techniques. In particular, the low-cut filter frequency, f_c, is an important parameter for displacement-based design and seismic performance assessment procedures, as it directly affects the displacement spectrum values at longer periods. There are numerous studies proposing various low-frequency filtering techniques that eliminate the low-frequency noise from the raw ground-motion records to obtain physically justifiable velocity and displacement time series [Ambraseys et al., 2004; Bommer and Elnashai, 1999; Boore et al., 2002; Skarlatoudis et al., 2003; Trifunac, 1971; Trifunac et al., 1973; Trifunac and Todorovska, 2001; Zaré and Bard, 2002] Of these numerous studies, some researchers suggested to choose filter cut-off using the signal to noise ratio [e.g., Skarlatoudis et al., 2003; Trifunac and Todorovska, 2001] whereas some techniques iteratively modified the low-cut filter frequency until the processed velocity and displacement waveforms appear to be physically reasonable [e.g., Bommer and Elnashai, 1999]. Recently, the variation of acceleration Fourier amplitudes at low and high frequencies is also considered to determine a physically justifiable f_c for removing the low-frequency noise from the raw accelerograms [e.g., Ambraseys et al., 2004; Zaré and Bard, 2002]. It should be noted that regardless of the filtering technique selected, it should not distort the important features of the record [Boore and Bommer, 2005].

[1] Earthquake Engineering Research Center, Middle East Technical University, 06531 Ankara, Turkey
Email : emrah.yenier@gmail.com
[2] Earthquake Research Department (ERD), General Directorate of Disaster Affairs, 06530 Ankara, Turkey
Email: zahide@deprem.gov.tr
[3] Earthquake Research Department (ERD), General Directorate of Disaster Affairs, 06530 Ankara, Turkey
Email: azeynel@deprem.gov.tr
[4] Earthquake Engineering Research Center, Middle East Technical University, 06531 Ankara, Turkey
Email: sakkar@metu.edu.tr

Using two-pass Butterworth filter and European ground-motion databank, Akkar and Bommer [2006] investigated the influence of low-cut filter frequency on the elastic displacement demands by considering the distinct behavior of the analogue and digital records associated with the influence of earthquake magnitude, soil type, viscous damping and filter order. They indicated that the usable period interval of displacement spectrum for digital records is considerably longer than those for the analogue records. They also stated that the increase in earthquake magnitude is associated with a longer usable period range for elastic displacement spectrum. Furthermore, it is found that, as far as the site conditions are concerned, the increase in the shear wave velocity profile of soil implies an increase in the influence of f_c on the elastic displacement spectrum, thus the usable period-band gets shorter relative to the selected f_c. As part of this study, Akkar and Bommer [2006] proposed a methodology for determining the low-cut filter frequency that is primarily based on (a) noise information revealed by the fixed trace of analogue records, (b) guidance of theoretical source spectrum together with the behavior of acceleration Fourier amplitude spectrum (FAS). In this procedure, item (a) is suggested whenever the fixed trace information of the analogue record is available. If this information is missing or if the records are digital, the procedure uses the option stated in item (b) to determine f_c. The details of the proposed technique are described in the succeeding sections of this paper.

The major objective of this study is to observe the similarities and differences in the low-cut filter frequencies determined by the above alternative approaches described in Akkar and Bommer [2006]. A total of 19 pairs of analogue ground-motion records (i.e., horizontal components perpendicular to each other) from Turkish ground-motion database with available fixed trace information are used to achieve the objectives of the study. The elastic and inelastic spectral displacements as well as peak ground-motion values are computed to see how f_c values determined from these approaches influence the long-period information revealed by the ground motions.

2. GROUND-MOTION DATA SET

A total of 19 analogue records with fixed trace information available for their horizontal components are processed according to the low-frequency filtering techniques explained in the next section. The original films that contain the horizontal acceleration waveforms and fixed traces are scanned using 600 dpi resolution and digitized by the SMA Scanview software [Kinemetrics, 1990]. The list of ground-motion records together with some important seismological features are presented in Table 1. All of the records listed in Table 1 belong to pre-2000 events from Turkey and the sensor type is the same for all recordings (SMA-1) except for the 19th record (SM-2). The records listed in Table 1 mostly belong to small or moderate magnitude events and the

Table 1: List of the ground-motions used in the study

Rec. #	Event		Magnitudes			Epicentral Distance (km)
	Date	Time (GMT)	M_W	M_S	M_B	
1	05/07/1983	12:01	6.1	6.1	5.5	81.52
2	05/07/1905	12:01	6.1	6.1	5.5	48.64
3	30/10/1983	04:12	6.6	6.9	6.1	34.48
4	04/08/1988	08:25			4.5	31.56
5	12/02/1991	09:54		4.6	4.8	38.52
6	06/11/1992	19:08	6.0	6.0	5.7	31.89
7	03/01/1994	21:00		4.8	5.0	67.7
8	24/05/1994	02:05	5.5	5.4	4.9	20.1
9	24/05/1994	02:18		4.9	5	19.89
10	13/11/1994	06:56	5.4	5.0	4.9	17.41
11	13/11/1994	07:13			4.3	11.68
12	13/11/1994	07:58		4.4	4.8	9.48
13	13/11/1994	08:15		4.5	4.8	27.17
14	21/01/1997	20:47	5.2	4.3	5	11.23
15	22/01/1997	17:57	5.7	5.4	5.4	109.89
16	25/10/1997	00:38			4.2	21.37
17	27/06/1998	13:55	6.2	6.2	5.8	32.07
18	27/06/1998	13:55	6.2	6.2	5.8	58.79
19	27/06/1998	13:55	6.2	6.2	5.8	95.92

epicentral distance of the records are mostly less than 100 km. Table 1 reveals that the body wave magnitudes, M_B, are available for all records whereas the moment magnitudes, M_W and surface wave magnitudes, M_S, for some of the records are missing. The body wave magnitudes used to estimate to the missing M_S and M_W values based on the relationships for various magnitude scales presented in Kramer (1996). This assumption is used while implementing Approach-II that is described in the next section.

3. DESCRIPTION OF DATA PROCESSING METHODOLOGIES

In this study, the ground-motion data set presented in Table 1 is processed using the two approaches presented by Akkar and Bommer [2006]. The following sub-sections describe these approaches in detail and present particular cases about their implementation to raw acceleration data. It should be noted that the common step in both approaches is removing the mean of whole accelerogram from the entire raw acceleration time series that can be considered as an initial baseline adjustment. The records that are obtained after the application of this step are referred to as "mean removed" records and they are filtered after determining f_c values in accordance with the methodologies described below. Two-pass, 4-pole/4-pole Butterworth filter is used during the filtering process resulting in phase distortionless ground-motion time series that reduce the sensitivity of oscillator vibration frequency to the low-cut filter frequency value. The peak ground-motion values and spectral quantities draw a more stable picture when acceleration time series are processed by phase distortionless filters [Boore and Akkar, 2003; Boore and Bommer, 2005]. The public open filtering software developed by Dr. David M. Boore from USGS is used in this paper (http://quake.wr.usgs.gov/ ~boore/software_online.htm).

3.1 Low-cut Filtering Using Fixed Trace Information (Approach-I)

This approach is fairly straightforward and it is suggested to be used whenever the fixed trace information on the original film is available [Akkar and Bommer, 2006]. The access to digitized fixed trace information is limited in most ground-motion recordings. Thus, the implementation of this approach is not common. The procedure simply makes use of the FAS ratios of the noise contaminated signal (i.e., mean removed acceleration trace) and the noise represented by the fixed trace. The Fourier amplitude spectrum ratio of these two time series is designated as "(signal+noise)/noise" or simply (S+N)/N. Boore and Bommer [2005] suggested that the low-frequency band of the signal where (S+N)/N values are less than 3 is dominated by the noise and these components should be removed from the signal. Akkar and Bommer [2006] also suggested this limit to determine the noise dominated frequency band. The application of this approach is shown in Figure 1 for the longitudinal component of the Rec. #1 (M_w=6.1) presented in Table 1. Figure 1a presents the FAS ratios of signal and noise (mean removed acceleration) to noise (fixed trace). A trend line (dashed gray line) is fitted to this ratio to compute the intersecting point with (S+N)/N=3 (dashed-two-dotted gray line). The intersection point approximately represents the limiting frequency dominated by noise and frequencies lower than this limiting value should be removed. Thus low-cut filter frequency determined for this particular case is f_c=3.46 Hz. This value is significantly high and removes a significant part of the frequency components from the ground-motion

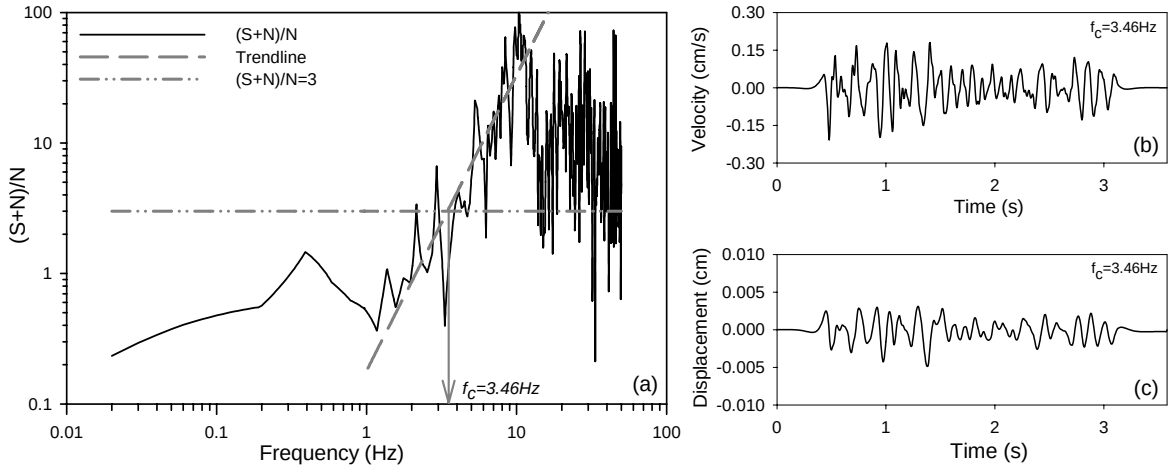

Figure 1: The (signal+noise)/noise ratio and the velocity and displacement time series of the acausally filtered record according to the f_c calculated using Approach-I

data. Figure 1b and 1c show the velocity and displacement traces computed using this f_c value, respectively. The variations of these time series can be accepted as physically rational that suggests the termination of filtering process for this particular record.

3.2 Low-cut Filtering Using the Guidance of Source Spectra of FAS (Approach-II)

Akkar and Bommer [2006] suggested the second approach for analogue recordings without fixed trace information or digital ground-motion data. This approach uses the guidance of acceleration FAS corner frequencies estimated from theoretical source spectra. Akkar and Bommer [2006] proposed the use of single-corner source spectrum model presented in Joyner and Boore [1988] and two-corner frequency model proposed by Atkinson and Silva [2000]. The use of theoretical source spectra would yield generic information about the theoretical frequency content of the records. The theoretical source spectra used in this approach require moment magnitude, M_W, to compute FAS corner frequencies. In this study, the relationship presented in Kramer (1996) is used to convert M_B values to M_W for the records that lack the moment magnitude values listed in Table 1. Note that the theoretical source spectra selected are among the representatives of few source spectrum models suggested in the literature. The reader is referred to Boore [2003] for a detailed review of source spectra that can also be incorporated to this approach. The approach suggests using a low-cut filter frequency lower than the FAS corner frequencies suggested by these two source spectra. The analyst starts with a candidate f_c that is lower than these theoretical FAS corner frequencies and then changes it iteratively if the processed displacement traces contain long-period fluctuations running along the total record length or they contain any other physically unjustifiable trend in the displacement waveforms such as very large displacements at the end of the record. Given these source spectra, the ground-motion data is considered as severely distorted when the iterative procedure yields significantly larger f_c values with respect to the theoretical FAS corner frequencies. For such cases the analyst may consider discarding the data from the database. Albeit the subjectivity of this approach due

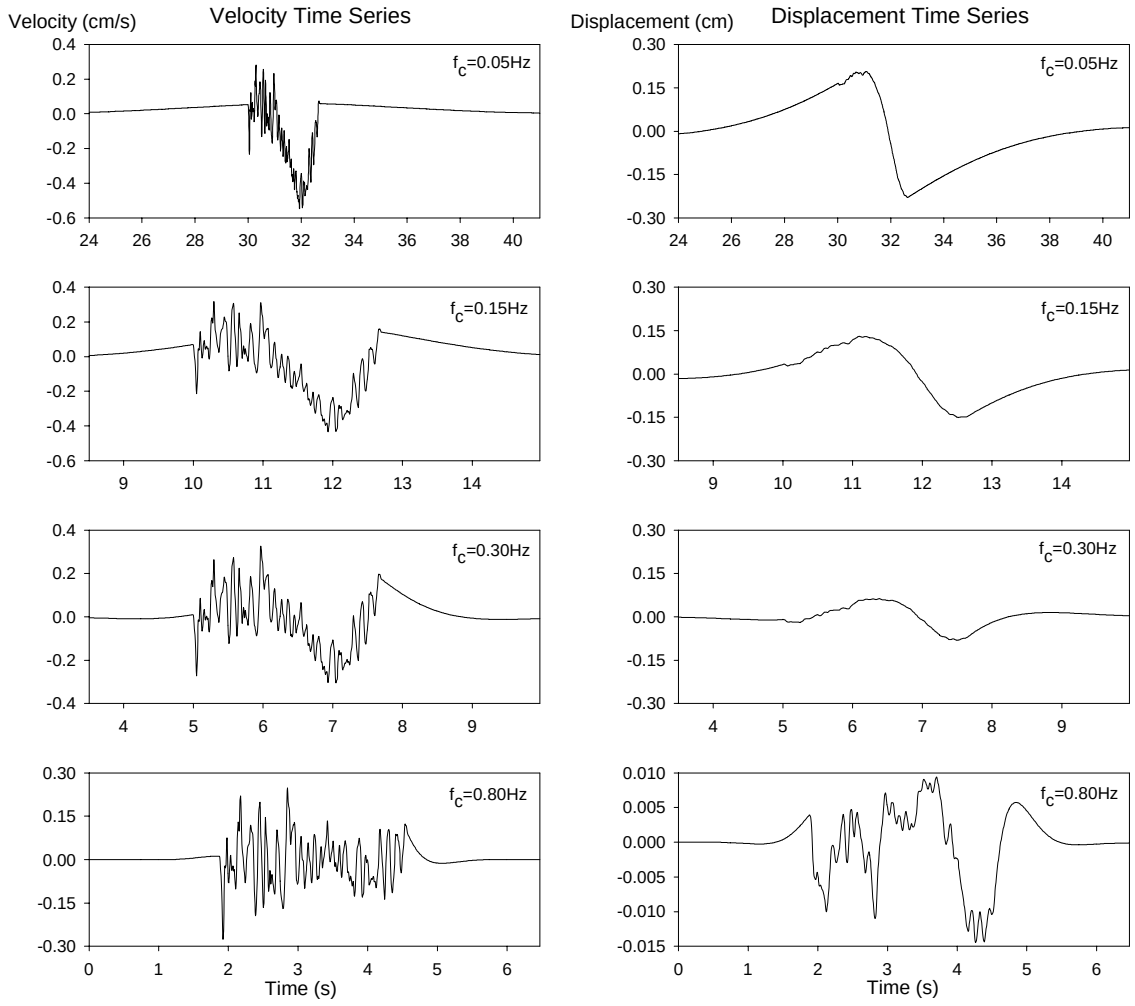

Figure 2: The velocity and displacement time series obtained for different f_c values when Approach-II was applied to the longitudinal component of Rec. #1. The different time axis scaling of the processed waveforms is due to the zero padding of acausal filtering used in the computations

to the choice of theoretical source spectra or the visual inspection of the processed ground-motion to finalize the iterations, it fairly describes the frequency content of the processed ground-motion after the filtering process.

Figure 2 presents the implementation of this approach for the ground-motion record used in Section 3.1. The single-corner source spectrum by Joyner and Boore [1988] results in a FAS corner frequency of 0.28 Hz (f_{JB88}) whereas the Atkinson and Silva [2000] spectrum suggests the FAS corner frequencies as 0.14 Hz ($f_{a,AS00}$) and 0.83 Hz ($f_{b,AS00}$) that control the finite-fault size and sub-fault sizes, respectively. The figure represents the low-cut filtered velocity and displacement time series for f_c=0.05 Hz, 0.15 Hz, 0.30 Hz and 0.80 Hz. The low-cut filter frequency, f_c=0.05 Hz, is significantly lower than the FAS corner frequencies suggested by the theoretical source spectra. The f_c value of 0.80 Hz represents practically the upper corner frequency for the theoretical source spectra suggested by Atkinson and Silva [2000]. The velocity and displacement time series presented in Figure 2 indicate that the time series filtered by f_c=0.80 Hz describes the most reasonable ground-motion variation with respect to the rest of the time series. The displacement time series obtained from other f_c values display a dominant long-period waveform that masks the actual particle displacement due to ground shaking. Figure 3 shows the acceleration FAS spectra of mean removed and filtered time series. This figure also displays the FAS corner frequencies suggested by the theoretical spectra used. The Fourier amplitudes of the time series filtered by f_c=0.80 Hz decay fairly faster than the scaled f^2 gradient at the lower frequency interval confirming the theoretical behaviour of acceleration FAS.

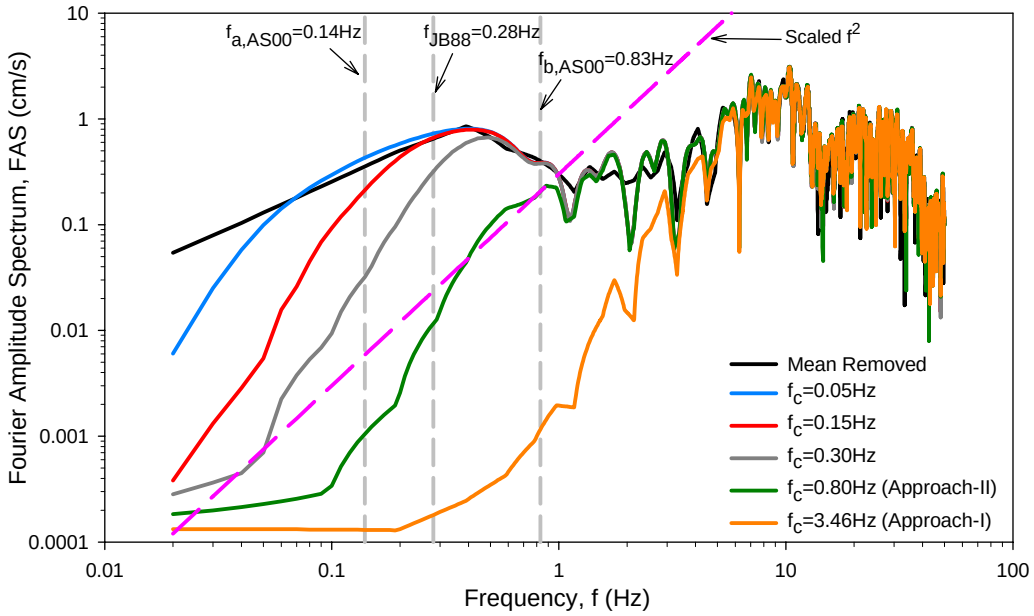

Figure 3: FAS of the filtered records for different low-cut frequencies and mean removed for the longitudinal component of Rec. #1

It should be noted that there is a significant difference between the f_c values computed using these two approaches. The approach that makes use of the fixed trace information (i.e., Approach-I) removes a significant amount of low-frequency information that is reflected clearly in the processed displacement time series. The next section presents detailed comparisons about how these two approaches affect the peak ground-motion values and spectral quantities for the ground motions processed in this study.

4. COMPARISON OF RESULTS

The low-cut filter frequencies computed from two approaches described in the previous section are compared in Figure 4. Figure 4a presents the scatter plots for f_c values computed by Approach-I ($f_{c,Approach-I}$) versus the f_c values of Approach-II ($f_{c,Approach-II}$). A straight line is fit to observe the relationship between the f_c values defined from these alternative schemes. The regression line clearly indicates that the f_c values determined from Approach-I are more conservative with respect to those computed by Approach-II. Most of the large f_c values determined by these alternative schemes pertain to the ground-motions recorded during small events ($M_W < 5$). This is presented explicitly in Figure 5 that shows the variation of computed filter cut-offs with respect to M_W. Thus, the low-frequency signal information that can be retrieved from small events recorded by analogue accelerograms is considerably limited. Figure 4b presents the scatter plots for filter cut-offs computed for the mutually perpendicular horizontal components separately (i.e., f_c values for longitudinal and transverse

components, $f_{c,L}$ and $f_{c,T}$, respectively). The scatters suggest that, regardless of the approach, the longitudinal and transverse component filter cut-offs are very similar to each other for most cases suggesting that the low-cut filter frequency for one horizontal component is almost valid for the mutually perpendicular other component.

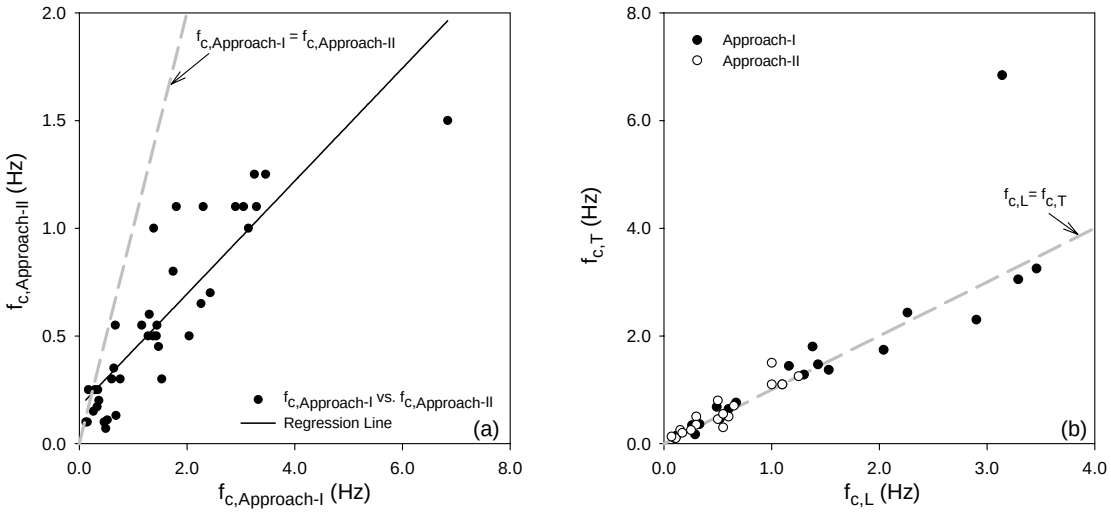

Figure 4: (a) scatter for $f_{c,\ Approach-I}$ vs. $f_{c,\ Approach-II}$, (b) scatter for f_c values computed for longitudinal and transverse components separately

The variation of computed filter frequencies by Approach-I and Approach-II with respect to M_W is demonstrated in Figure 5. The theoretical FAS corner frequencies (f_{JB88}, $f_{a,AS00}$ and $f_{b,AS00}$) are also illustrated in this plot to see if the frequency content of the records is distorted severely. It should be noted that the f_c values determined from the alternative approaches decrease with increasing magnitude that follow a similar trend suggested by the corner frequencies of the theoretical source spectra. The low-cut filter frequencies determined by Approach-I are generally larger than the theoretical FAS corner frequencies suggesting that Approach-I is more likely to remove a large portion of the low-frequency content of the signal. This observation is particularly true if the theoretical FAS corner frequencies presented are accepted to mimic the actual frequency content of the ground-motion. The low-cut filter frequencies suggested by Approach-II generally stay within the boundaries of FAS corner frequency values proposed by Atkinson and Silva [2000]. Filter cut-offs that are closer to the upper corner frequency $f_{b,AS00}$ indicate the severe removal of low-frequency ground motion components. The analyst should seriously consider discarding the processed ground motions filtered by f_c values that are either close or above the $f_{b,AS00}$ boundary.

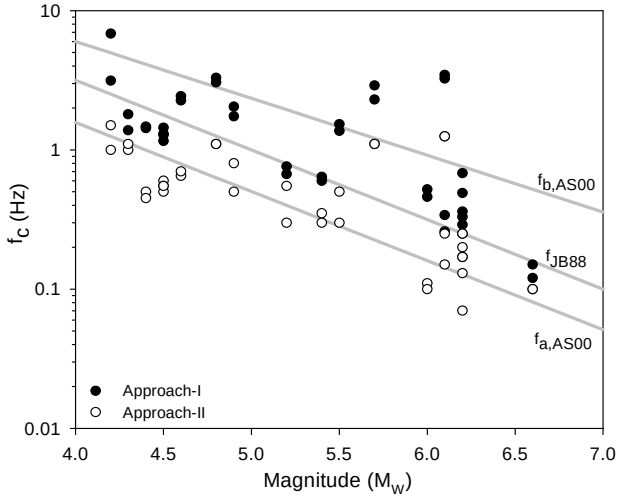

Figure 5: Variation of low-cut frequencies with respect to moment magnitude

Figure 6 shows the variation of peak ground acceleration, velocity and displacement (PGA, PGV and PGD, respectively) values computed from the processed records using Approach-I and -II. The influence of different f_c values on the computed peak ground-motion values from processed records is pronounced for PGD. The changes

in f_c is due to alternative approaches influence the PGV values to a lesser extent. The PGA values computed from these two approaches are almost the same indicating that the peak ground acceleration values is the least affected parameter from filtering. The plots in Figure 6 show that PGD values computed from Approach-II are greater than those computed from Approach-I. This is expected as f_c values derived from Approach-I are mostly greater than those of Approach-II and they remove a significant portion of low frequency components from the processed ground motions.

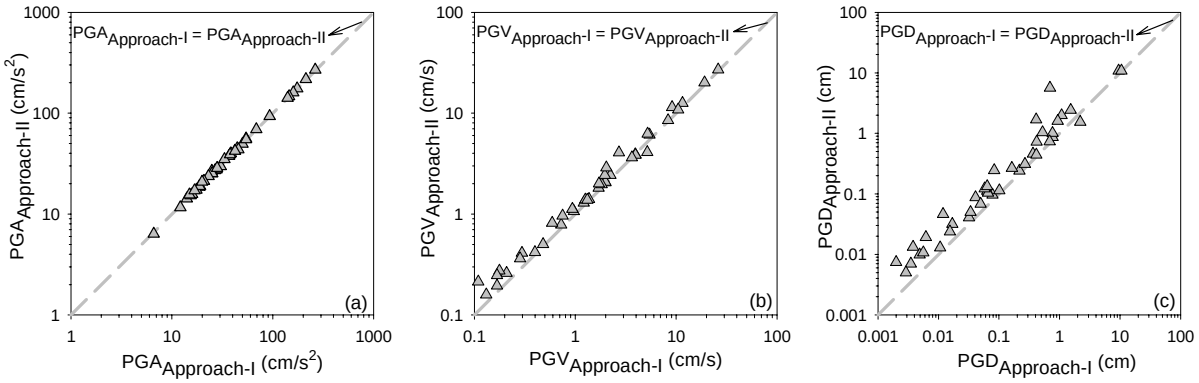

Figure 6: Effect of low-cut filter frequencies on peak ground-motion ordinates

Figures 7 to 9 show the influence of f_c values determined from the alternative approaches on elastic and inelastic spectral displacements that are computed for the longitudinal component of Rec. # 17. The low-cut frequency values determined by Approach-I and –II are 0.49 Hz and 0.07 Hz for this particular record, respectively. Spectral displacements promote the low-frequency components of the ground motions and describe the influence of f_c computed from the alternative approaches in a clearer manner. Moreover, reliable spectral displacement ordinates are essential for the most recent analysis techniques that are used for assessing the seismic vulnerability of structures. Figure 7 presents the comparison for elastic spectral quantities ($S_{d,e}$) whereas Figures 8 and 9 display similar comparisons for inelastic spectral displacement ordinates ($S_{d,i}$).

The comparison for elastic spectrum presented in Figure 7 reveals that both approaches would yield similar spectral displacement ordinates for oscillator frequencies greater than 1 Hz. The departure between two approaches is significant particularly for vibration frequencies lower than 0.5 Hz (i.e., $T \geq 2$ s). This illustrates how the low frequency content of the ground-motion record is reduced by the Approach-I. It should be noted that the influence of filter cut-off determined from Approach-I on $S_{d,e}$ starts at a higher vibration frequency ($f_c \approx 1$ Hz) that is consistent with the observations highlighted by Akkar and Bommer [2006]. In other words, the low-cut filter frequency influence on elastic spectral displacements starts at relatively higher vibration frequencies with respect to the chosen f_c value.

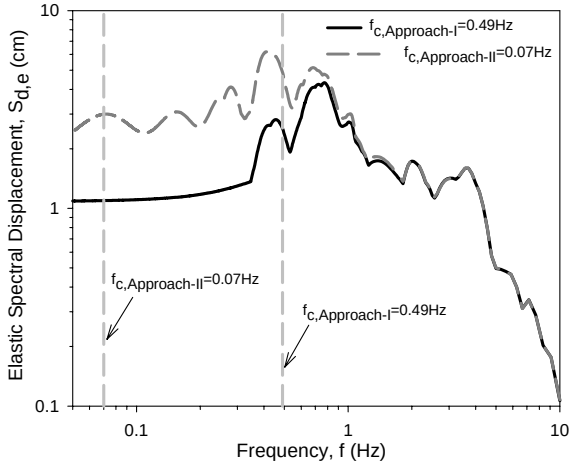

Figure 7: Influence of low-cut filter frequency determined from Approach-I and Approach-II on elastic spectral displacement ordinates for the longitudinal component of Rec. #17

Figures 8 and 9 present a similar comparison as in the case of Figure 7 for inelastic spectral displacements computed for constant strength and constant ductility, respectively. The constant strength displacement spectra are plotted for lateral strength ratio, R, that represents the lateral strength that maintains the system elastic

normalized by the yield strength of the system. The constant ductility displacement spectra are plotted for displacement ductility ratio, μ, that is described as the maximum inelastic displacement of the system divided by its yield displacement. The plots in Figure 8 represent constant strength displacement spectra for R=2, 4, 6 and 8 that simulate different levels of inelasticity. The spectral displacements for R=2 represents a strong system whereas the inelastic spectral displacements for R=8 represents a weaker system whose yield strength is 1/8th of the corresponding elastic strength. The inelastic displacement spectra presented in Figure 9 are plotted for μ=2, 4, 6 and 8 similar to the previous figure where different μ represents different levels of inelasticity. The increase in μ refers to an increase in the level of inelasticity. Similar to the observations made for elastic spectral displacement ordinates the discrepancy due to different f_c values computed from Approach-I and -II becomes clearer at lower frequency values. The spectral displacements computed from the ground motion processed by Approach-II are twice larger than those of Approach-I at lower frequencies since this approach yields a significantly smaller f_c value resulting in a lesser reduction in the low-frequency content of the ground motion. A remarkable difference with respect to the elastic behavior is that the increase in the level of inelasticity (i.e., higher R and μ values) implies a comparable difference in the inelastic spectral displacement ordinates computed from these alternative approaches. This indicates that the inelastic oscillator behavior is more sensitive to the changes in f_c. Another interesting observation from Figures 8 and 9 is that the decreasing difference between the inelastic spectral displacement ordinates computed from Approach-I and -II for increasing level of inelasticity (i.e., increasing R or μ) for intermediate frequency interval (i.e. 0.5Hz – 1.0 Hz). In other words, the observed differences for the lower constant R or μ inelastic spectral displacements within this frequency band due to different filter cut-offs diminish as R or μ increases. It should be noted that the observations presented in this paper are based on few records. They are not sufficient to explain the complex interaction between the low-cut filter frequency, nonlinear oscillator response and salient seismological features that play a role in the ground motion behavior.

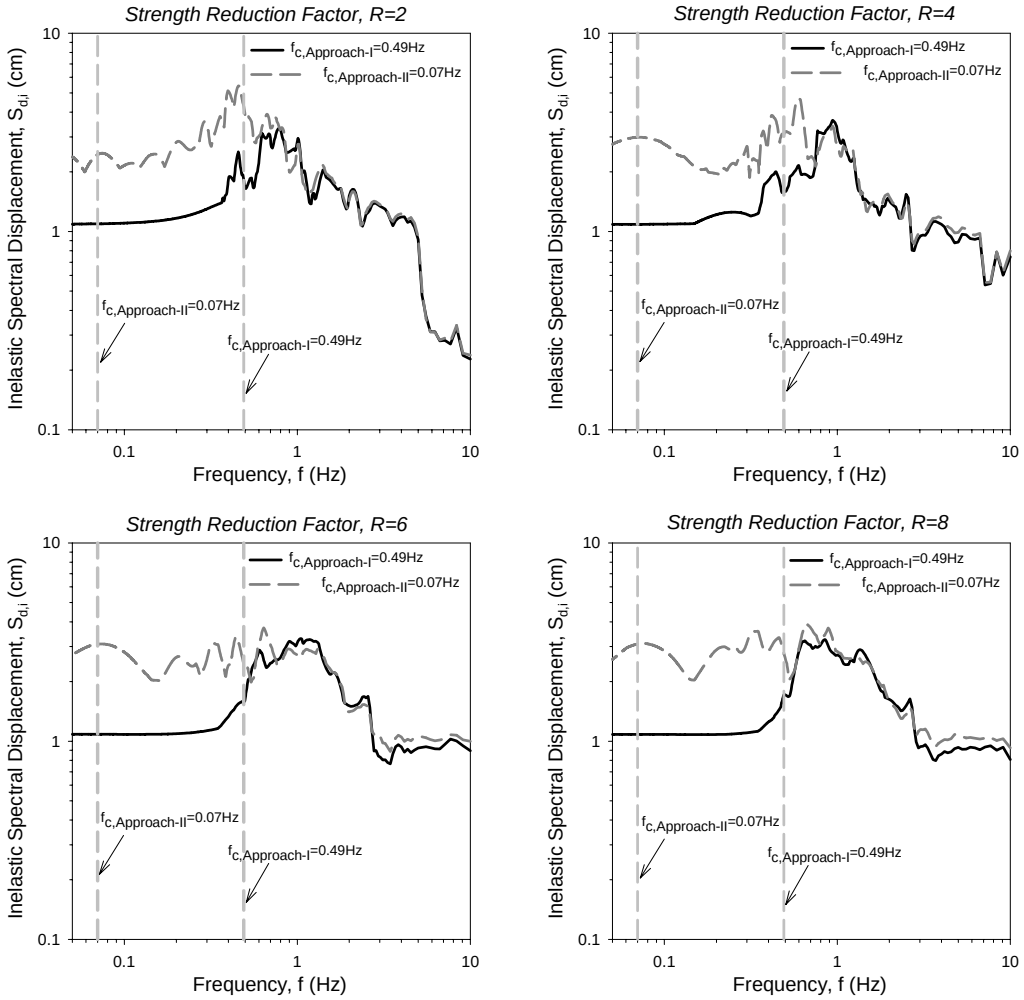

Figure 8: Influence of low-cut filter frequency on inelastic spectral displacement ordinates for constant strength displacement spectrum for the longitudinal component of Rec. #17

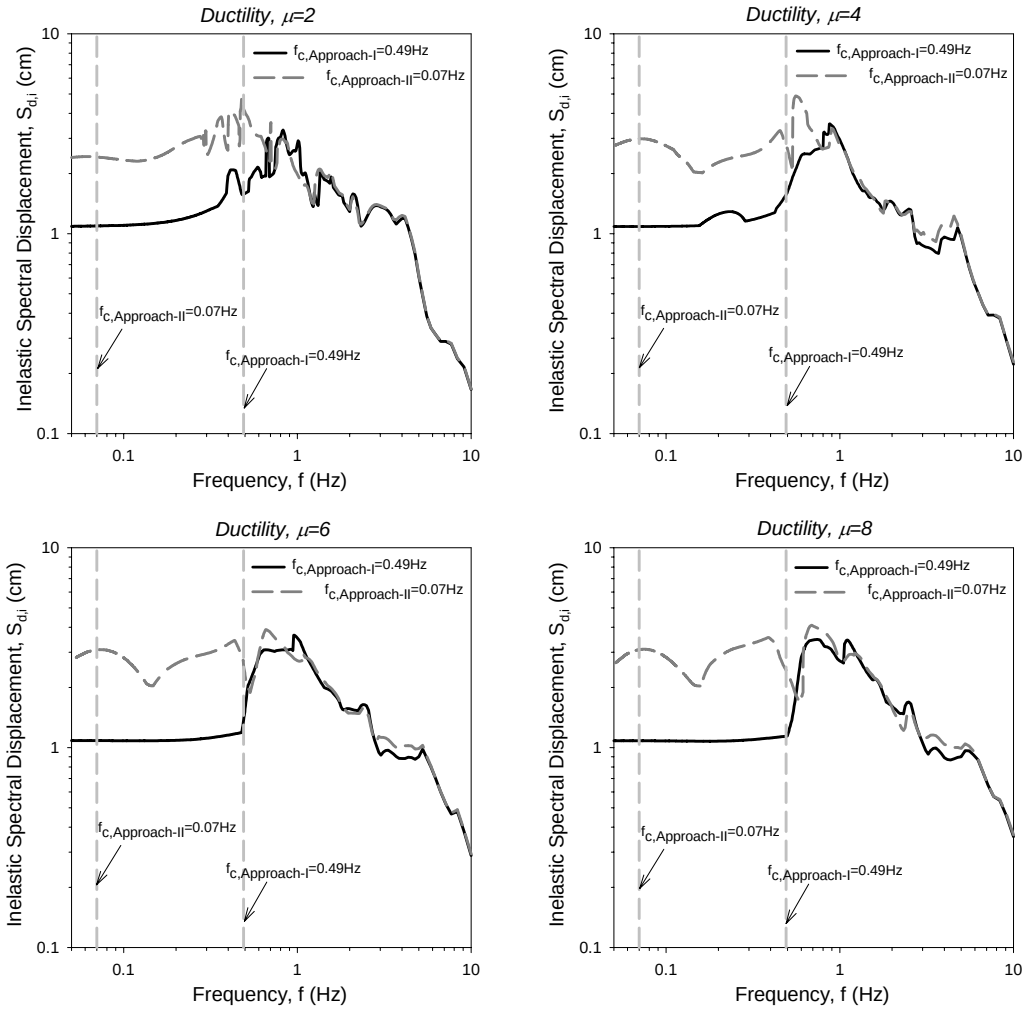

Figure 9: Influence of low-cut filter frequency on inelastic spectral displacement ordinates for constant ductility displacement spectrum for the longitudinal component of Rec. #17

5. SUMMARY AND CONCLUSIONS

Horizontal components of 19 analogue records with available fixed trace information from Turkish strong ground-motion database are processed using two approaches that define alternative low-cut filter frequencies. Of these methods, Approach-I, makes use of FAS ratios of the noise contaminated signal and the noise represented by the fixed trace to define the low-cut filter frequency. The other method, Approach-II, determines f_c by an iterative scheme associated with the guidance of acceleration FAS corner frequencies calculated from the theoretical source spectra. Two-pass, 4-pole/4-pole Butterworth filter is used in both approaches to obtain zero-phase ground-motion time series. The results are compared in terms of f_c calculated from these two approaches. It is observed that filter cut-offs determined from Approach-I are considerably larger than those computed from Approach-II. This might be the indication for the removal of significant portion of low frequency components from the ground motion data. The influence of f_c determined from these alternative approaches is minimum on PGA and maximum for PGD. The low-cut filter frequency determined from Approach-I results in significantly lower spectral displacement values with respect to those of Approach-II both for linear and nonlinear oscillator response at the lower vibration frequencies. For inelastic oscillator response, the discrepancy between these alternative approaches also starts from higher vibration frequencies emphasizing the sensitivity of nonlinear behavior to the changes in f_c. The influence of f_c determined from these alternative approaches on inelastic spectral displacements varies for different levels of inelasticity indicating the complexity of this issue.

6. ACKNOWLEDGEMENTS

This study is funded by the Scientific and Technological Research Council of Turkey under Award No. 105G016.

7. REFERENCES

Akkar S., Bommer JJ. (2006), Influence of long-period filter cut-off on elastic spectral displacements, E*arthquake Engineering and Structural Dynamics*, 35, (in press).

Atkinson, G.M., Silva, W. (2000), Stochastic modeling of California ground motions, *Bulletin of the Seismological Society of America*, 90:255-274.

Bommer, J.J., Elnashai, A.S. (1999), Displacement spectra for seismic design, *Journal of Earthquake Engineering*, 3,1-32.

Boore, D.M., Stephens, C.D. and Joyner, W.B. (2002), Comments on baseline correction of digital strong motion data: examples from the 1999 Hector Mine, California, earthquake, *Bulletin of the Seismological Society of America*, 92,1543-1560.

Boore, D. M. (2003), Simulation of ground motion using the stochastic method, *Pure and Applied Geophysics* 160, 635-675.

Boore, D.M., Akkar, S. (2003), Effect of causal and acausal filters on elastic and inelastic response spectra, *Earthquake Engineering and Structural Dynamics* , 32,1729-1748.

Boore, D.M., Bommer, J.J. (2005), Processing of strong-motion accelerograms: needs, options and consequences, *Soil Dynamics and Earthquake Engineering*, 25:93-115.

Joyner, W.B., Boore, D.M. (1988), Measurement, characterization, and prediction of strong ground motion, *Earthquake Engineering and Soil Dynamics II, Proceedings of American Society of Civil Engineers Geotechnical Engineering Division Specialty Conference*, Park City, Utah, 43-102.

Kinemetrics (1990), SMA Scanview: Scanner-based film accelerogram digitization system user's manual, *Document 301561*, Kinemetrics, Pasadena, California.

Kramer, S.L. (1996), Geotechnical Earthquake Engineering, *Prentice-Hall*, New Jersey.

Lee, V.W., Trifunac, M.D. (1990), Automatic digitization and processing of accelerograms using PC., *Report 90-03*, Department of Civil Engineering, University of Southern California, Los Angeles.

Skarlatoudis, A.A., Papazachos, C.B. and Margaris, B.N. (2003), Determination of noise spectra from strong motion data recorded in Greece, *Journal of Seismology*, 7, 533-540.

Trifunac, M.D. (1971), Zero baseline correction of strong-motion accelerograms, *Bulletin of the Seismological Society of America,* 61,1201-1211.

Trifunac, M.D., Udwadia F.E. and Brady AG. (1973), Analysis of errors in digital strong-motion accelerograms, *Bulletin of the Seismological Society of America*, 63,157-187.

Trifunac, M.D., Todorovska, M.I. (2001), A note on the usable dynamic range of accelerographs recording translation, *Soil Dynamics and Earthquake Engineering*, 21,275-286.